tvst

https://doi.org/10.1167/tvst.8.6.45

Article

Chromatic Full-Field Stimulus Threshold and Pupillography as Functional Markers for Late-Stage, Early-Onset Retinitis Pigmentosa Caused by *CRB1* Mutations

Krunoslav T. Stingl[1], Laura Kuehlewein[1], Nicole Weisschuh[1], Saskia Biskup[2], Frans P. M. Cremers[3], M. Imran Khan[3], Carina Kelbsch[1], Tobias Peters[1], Marius Ueffing[1], Barbara Wilhelm[1], Eberhart Zrenner[1,4], and Katarina Stingl[1]

[1] Center for Ophthalmology, University of Tübingen, Tübingen, Germany
[2] Praxis für Humangenetik Tübingen, Tübingen, Germany
[3] Department of Human Genetics, Radboud University Medical Center and Donders Institute for Brain, Cognition and Behaviour, Nijmegen, the Netherlands
[4] Werner Reichardt Center for Integrative Neuroscience, University of Tübingen, Tübingen, Germany

Correspondence: Tobias Peters, Center for Ophthalmology, University of Tübingen, Elfriede-Aulhorn-Str. 7, 72076 Tübingen, Germany. e-mail: tobias.peters@stz-eyetrial.de

Received: 8 February 2019
Accepted: 30 September 2019
Published: 20 December 2019

Keywords: retinitis pigmentosa; *CRB1* mutation; functional marker

Citation: Stingl KT, Kuehlewein L, Weisschuh N, Biskup S, Cremers FPM, Khan MI, Kelbsch C, Peters T, Ueffing M, Wilhelm B, Zrenner E, Stingl K. Chromatic full-field stimulus threshold and pupillography as functional markers for late-stage, early-onset retinitis pigmentosa caused by *CRB1* mutations. Trans Vis Sci Tech. 2019;8(6):45, https://doi.org/10.1167/tvst.8.6.45

Purpose: Mutations in the *CRB1* gene cause early-onset retinal degeneration (EORD). Clinical disease progression markers, such as visual fields or electrophysiology, are not reliably measurable in most patients to follow the retinal function in patients with *CRB1*-mutations.

Methods: Ten patients (five females, five males; age 22–56 years) with EORD caused by *CRB1* mutations were examined in a cross-sectional manner using best corrected visual acuity (BCVA), perimetry, full-field and multifocal electroretinography, full-field stimulus threshold (FST), and pupillography to red and blue light. Disease duration was defined as the difference between the age at the first symptoms to the age at examination in years.

Results: BCVA was quantifiable in six patients and ranged from light perception to 20/50. The visual field was measurable only in three patients who had the shortest disease duration. Full-field and multifocal electroretinography were not measurable in any patient. FST to blue and red light were measurable in all patients except the one with the longest disease duration; the thresholds ranged from −16.7 to 1.5 dB for red light and from −40.2 to 2.5 dB for blue light (0 dB = 0.01 cd.s/m^2) and showed correlations with disease duration ($r = 0.87$ for blue, $r = 0.65$ for red, $r = 0.8$ for blue–red difference). The maximal relative pupil constriction amplitude (MRA) showed low or no correlations with disease duration ($r = -0.55$ for blue, $r = -0.3$ for red light); the blue–red difference in the post-illumination pupil responses (PIPR) showed no correlation with disease duration ($r = -0.05$). Compared to healthy eyes, the MRA to red and blue light was significantly decreased ($P < 0.001$) and the blue–red PIPR difference was significantly increased ($P = 0.003$).

Conclusions: FST features a valid clinical marker in late-stage early-onset retinitis pigmentosa caused by *CRB1* mutations correlating with disease duration. This indicates the potential as a progression marker of disease. The pupil responses to full-field chromatic stimuli show significant differences from the normal population: the remaining responses, although reduced, indicate a partially preserved inner retinal function despite severe photoreceptor dysfunction.

Translational Relevance: The functional measurements presented in this study present a valid clinical progression marker in late-stage early onset retinitis pigmentosa caused by biallelic *CRB1* mutations. Additionally, they can be used as outcome measures for safety and efficacy in clinical therapy trials.

Introduction

Mutations in the *Crumbs Homolog 1* (*CRB1*) gene typically are associated with early-onset retinal degeneration (EORD) or Leber congenital amaurosis (LCA) with an autosomal recessive inheritance,[1] the RP12 subform of retinitis pigmentosa (RP),[2] but also with macular degeneration.[3]

CRB1 is a human homologue of the *Drosophila melanogaster* gene coding for protein crumbs (crb) expressed in the retina and brain.[2] In *Drosophila,* the crb protein has been described to take part in a protein complex essential for proper polarity of peripheral neurons. In the mouse retina, *CRB1* is involved in photoreceptor morphogenesis, being localized in Mueller cells and photoreceptor inner segments—here mainly localized at the outer limiting membrane.[4] Mammalian CRB proteins (CRBs) comprise several isoforms, with yet poorly defined individual functions. Although *CRB1* and its loss of function have been investigated in depth in mouse models, knowledge of the human CRB protein in the context of human retinal development and function remains scarce.[5,6] Mammalian CRB is found in the outer limiting membrane, microvilli of Mueller cells, Henle's fibers of Mueller cells in close contact with photoreceptor cells as well as in their inner segments[7] Although the exact role of *CRB1* in humans remains a matter of discussion, clinical findings in patients with *CRB1* mutations indicate that it is important for the morphogenesis and maturation of the retina.[1,8] Interestingly, patients with retinal degenerations due to biallelic *CRB1* mutations have a relatively thick retina unlike other inherited retinal degenerations studied.[8]

The proper assessment of the clinical phenotypes of patients with inherited retinal degenerations caused by *CRB1* mutations appears challenging, because these phenotypes present as variable, even for the same type of homozygous mutations.[9] Nevertheless, some common typical patterns are identified. Patients most frequently present with LCA or an early-onset RP with the first symptoms in early childhood; the average age of first symptoms is 7 (range, 0–28 years).[9,10] Specifically, a nummular pattern of retinal pigmentation rather than bone-spicula pigment deposits, thickening of the retina with abnormal layering resembling an immature human retina, hypermetropia, Coats-like exudations, and paravenous pigmentation progressing into chorioretinal atrophy are further morphologic aspects associated with the *CRB1* phenotype.[1,8,9,11,12] Additionally, cystoid macular edema has been observed frequently in these patients. A distinct phenotype associated with *CRB1* mutations is cone-rod dystrophy with cystoid macular edema manifesting first in early childhood; the macular edema is pronounced and can be the first clinical finding in children mimicking other pediatric problems in ophthalmology, such as uveitis or X-linked retinoschisis.[13–15] A recent study also reported a third phenotype of autosomal recessive *CRB1*-associated retinal degeneration due to the presence of the in-frame deletion variant c.498_506del, p.(Ile167_Gly169del) in the homozygous or compound heterozygous state, leading to macular dystrophy.[3]

Due to early-onset of the degeneration, functional findings frequently are not measurable in young adulthood; subjective tests, such as visual fields, reveal concentric narrowing to less than 10° in early age. The best corrected visual acuity has been analyzed in the follow-ups of up to 45 years in 30 patients showing visual loss starting usually in the first decade with very variable progression rates involving temporary plateau phases.[9] Despite the very different progression rates based on visual acuity measures interindividually, the progression shows a symmetrical pattern in both eyes of individual patients.[9] Objective measures of the retinal function, such as responses from cones and rods, are not detectable on the full-field electroretinography in most patients.[1,9,10]

To search for valid functional progression markers for the course of early-onset RP caused by *CRB1* mutations, we examined patients with standard functional retinal diagnostics and full-field stimulus threshold measurement, as well as pupillary responses to blue and red light.

Materials and Methods

Clinical Investigations

Twelve patients (six females, six males; mean age, 37.8 ±14.3 years; range, 22–68 years) with early-onset RP caused by biallelic mutations in *CRB1* were examined at the Center for Ophthalmology, University of Tübingen, Germany.[16] Two patients were excluded from the analysis group due to glaucoma, which could bias the results from functional diagnostics.

As the control group for pupillographic data, we used 10 healthy age-matched subjects (age, 36.68 ± 13.97) from a previously reported larger cohort.[17]

All functional measurements were performed on both eyes. The research followed the tenets of the Declaration of Helsinki and informed consent was obtained from the subjects after explanation of the nature and possible consequences of the study. The protocol was approved by the Ethics Committee of the University Hospital of Tübingen.

The clinical examination included a detailed medical history, best corrected visual acuity (BCVA) testing using Early Treatment of Diabetic Retinopathy Study (ETDRS) charts and the Berkeley residual vision test (BRVT)in the low and very low vision range,[18] kinetic perimetry (Octopus 900; Haag-Streit International, Wedel, Germany), slit-lamp examination, fundus examination in mydriasis, full-field and multifocal electroretinography according to International Society for Clinical Electrophysiology of Vision (ISCEV) standards with an Espion E2/E3 (Diagnosys LLC, Cambridge, UK), and dark-adapted full-field scotopic threshold with blue and red light (FST; Diagnosys LLC, Cambridge, UK) with 0 dB set to 0.01 cds/m^2. The patients were dark-adapted for 20 minutes, based on ISCEV recommendations for scotopic full-field electroretinography (ERG). All ophthalmologic examinations were performed on both eyes.

For the FST examinations, the threshold values were averaged for both eyes per subject for the red and blue light measurements. Furthermore, the difference in the blue–red threshold as an indicator of rod-based vision[19] was calculated for each eye and averaged per subject.

Pupillary responses to red (28 lux [lx]; peak, 606 nm; 0.4 μW/cm^2/nm; full width at half maximum [FWHM], 12 nm) or blue (28 lx; peak, 426 nm; 19.5 μW/cm^2/nm; FWHM, 21 nm) light were examined in a consensual manner in a completely darkened room without previous dark adaptation. The selected eye was stimulated with 28 lx bright light (red or blue, stimulus duration 4 seconds) using a color light emitting diode (LED) stimulator (CH Electronics, Bromley, UK). The pupil light reaction of the fellow eye was recorded using infrared pupillometry (Compact Integrated Pupillograph CiP; AMTech, Dossenheim, Germany) over a period of 16 seconds including a prestimulus time of 5 seconds. Changes in the pupil diameter were recorded at a sampling frequency of 250 Hz. All pupillograms were analyzed offline. Blink artifacts were removed semiautomatically using a customized software for analysis of pupillographic data written in MATLAB (MATLAB 2017b; MathWorks, Inc., Natick, MA). Read-out parameters were the maximal relative amplitude (MRA) and post illumination pupil response (PIPR). MRA (in percent) was calculated as MRA = 1 − the maximal pupil constriction amplitude / baseline pupil diameter. PIPR was calculated as a sum of the relative amplitudes from 2 seconds after stimulus to the end of the recording time (5 seconds after stimulus) and was normalized by the time. The difference in PIPR between blue and red light stimulation (blue–red) was calculated as an indicator for the inner retinal function (see prior report[20] for detailed description).

Genetic Investigations

Among the 10 patients enrolled in this study, one was analyzed using conventional Sanger sequencing of all coding exons of the *CRB1* gene. One patient was analyzed using a targeted panel-based next-generation sequencing approach designed at the Department of Human Genetics, Radboud University Medical Center, Nijmegen, The Netherlands.[21] The remaining eight patients were analyzed using a panel-based sequencing approach in a diagnostic setting (Cegat GmbH and Praxis für Humangenetik, Tübingen, Germany). Variants were confirmed and family members were analyzed using conventional Sanger sequencing of the respective exons.

The potential pathogenicity of the missense changes identified in this study was assessed using four online prediction software tools, SIFT (available in the public domain at http://sift.bii.a-star.edu.sg/),[22] PolyPhen-2 (available in the public domain at http://genetics.bwh.harvard.edu/pph2/),[23] Mutation Taster (available in the public domain at www.mutationtaster.org/),[24] and Provean (available in the public domain at http://provean.jcvi.org/).[25]

Results

Clinical Findings

Ten patients (5 males, 5 females; mean age, 34.4 ± 11.9 years; range 22–56 years) with two *CRB1* variants were included in the data analysis. Disease duration varied between 17 and 56 years (average, 32 ± 12.13 years). Age at first symptom onset was within the first 6 years in all patients (average age, 2.4 years) based on reports from the medical history. The clinical findings are summarized in Table 1.

Visual acuity was measurable in six patients; in two of them, only one eye was measurable with the second eye having only light (CRB1-09) or hand motion (CRB1-13) perception. After converting the BCVA

Table 1. Overview of the Clinical Findings in Patients With Early-Onset RP Caused by *CRB1* Mutations

	CRB1 Variants	Reference (PMID)	MAF	Segregation Performed	Sex	Age at Onset	Age at Visit	Disease Duration
CRB1-01	c.2230C>T/*P*.R744* hom	25323024	0.00001221	Yes	M	0	24	24
CRB1-02	c.2308G>A/*P*.G770S hom	27113771	0.00002036	No	F	6	47	41
CRB1-04	c.803_806del/*P*.S268Nfs*33 het c.2234C>T/*P*.T745M het	This study 10508521	None 0.00006506	Yes	F	0	34	34
CRB1-05	c.733del/*P*.A245Pfs*57 het c.1914G>T/*P*.S638S het	This study	None	Yes	F	5	26	21
CRB1-09	c.407G>A/*P*.C136Y het c.1465G>T/*P*.E489* het	26766544	0.000004079 None	Yes	F	4	48	44
CRB1-10	c.2248G>A/*P*.G750S hom	23591405	None	Yes	F	0	56	56
CRB1-12	c.2498G>A/*P*.G833D het c.3442T>C/*P*.C1148R het	23077403 24618324	None	Yes	M	2	22	20
CRB1-13	c.506del/*P*.G169Vfs*37 het c.3086T>A/*P*.V1029E het	23591405 This study	0.000008127 None	Yes	M	1	40	39
CRB1-15	c.2843G>A/*P*.C948Y hom	10508521	0.0002027	Yes	M	1	25	24
CRB1-16	c.2843G>A/*P*.C948Y hom	10508521	0.0002027	Yes	M	5	22	17

Age at onset of the first symptoms, age at visit and disease duration (defined as the difference of the age at visit and the age of first symptoms) are expressed in years. Hom, homozygous; het, heterozygous; PMID, PubMed ID; MAF, minor allele frequency; R, right; L, left; n.m., not measurable; FC, finger counting; HM, hand movement perception; LP, light perception without light projection; f, female; m, male.

Table 1. Extended

	BCVA (decimal)			Full Field		FST in dB (0 dB = 0.01 cd/m^2)				
	R	L	Visual Field	ERG	mfERG	f	Red L	Blue R	Blue L	Pupillography
CRB1-01	FC	FC	n.m.	n.m.	n.m.	−2.3	−4.5	−28.0	−29.0	Performed
CRB1-02	LP	LP	n.m.	n.m.	n.m.	−0.5	−1.2	−8.0	−12.0	Performed
CRB1-04	0.3	0.4	10°	n.m.	n.m.	−11.0	−12.6	−11.9	−17.0	Performed
CRB1-05	0.5	0.1	<5° central and periph. Islands	n.m.	n.m.	−9.6	−12.9	−31.6	−37.7	Performed
CRB1-09	LP	0.025	n.m.	n.m.	n.m.	−2.6	−3.7	−13.9	−16.9	Performed
CRB1-10	LP	LP	n.m.	n.m.	n.m.	n.m.	n.m.	n.m.	n.m.	n.m. (nystagmus)
CRB1-12	0.01	0.025	L <5° central	n.m.	n.m.	−7.6	−10.8	−30.3	−35.1	Performed
CRB1-13	HM	0.005	n.m.	n.m.	n.m.	0.8	1.5	2.5	0.4	n.m. (nystagmus)
CRB1-15	LP	LP	n.m.	n.m.	n.m.	−1.8	−3.3	−16.3	−19.8	Performed
CRB1-16	0.05	0.25	Ring scotoma	n.m.	n.m.	−16.7	−16.5	−40.2	−39.7	Performed

into logMAR values and estimating the logMAR of low-vision BCVA based on the previous research of Lange et al.,[26] we found a significant correlation in BCVA with the thresholds for red FST ($r = 0.89$, $P = 0.008$). Significant correlations were not found in BCVA for the blue FST threshold or for the pupillographic results.

The visual field was measurable in only three patients who had the shortest disease duration at presentation. They showed a classic ring scotoma (with an irregular central visual field of 10°–20°) for the patient with the shortest disease duration of 17 years, and a visual field constriction to <5° in two patients with disease duration of 20 and 21 years, respectively.

Full-field and multifocal electroretinography according to ISCEV standards showed no measurable responses in all patients. Full-field scotopic threshold

Table 2. Assessment of the Pathogenicity of the Missense Variants Identified in This Study

Variant	Mutation Taster	Polyphen	SIFT	Provean
c.407G>A/*P*.C136Y	Disease causing (0.99)	Probably damaging (1.0)	Damaging (0.0)	Deleterious (−8.26)
c.2234C>T/*P*.T745M	Disease causing (0.99)	Probably damaging (1.0)	Damaging (0.0)	Deleterious (−4.85)
c.2248G>A/*P*.G750S	Disease causing (0.99)	Probably damaging (0.99)	Damaging (0.0)	Deleterious (−5.47)
c.2308G>A/*P*.G770S	Disease causing (0.99)	Probably damaging (1.0)	Damaging (0.0)	Deleterious (−5.48)
c.2498G>A/*P*.G833D	Disease causing (0.99)	Probably damaging (0.99)	Damaging (0.0)	Deleterious (−6.34)
c.2843G>A/*P*.C948Y	Disease causing (0.99)	Probably damaging (0.99)	Damaging (0.0)	Deleterious (−9.66)
c.3086T>A/*P*.V1029E	Disease causing (0.99)	Probably damaging (0.99)	Damaging (0.0)	Deleterious (−5.21)
c.3442T>C/*P*.C1148R	Disease causing (0.99)	Probably damaging (1.0)	Damaging (0.0)	Deleterious (−10.90)

to blue and red light was measurable in all patients except the one with the longest disease duration of 56 years (the patient could not see any light in the FST test). Pupillary responses were measurable in eight patients; the reason for nonrecordable pupillary responses in the two remaining patients was severe nystagmus. Baseline pupil sizes were 5.4 ± 0.6 and 5.5 ± 0.68 mm for red and blue light responses, respectively, in the patient group and 7.0 ± 0.47 and 6.9 ± 0.53 mm, respectively, in the control group. The pupil baselines were significantly smaller in patients than in the controls for red and blue light conditions ($P < 0.001$).

Correlations With Disease Duration

Visual acuity was not measurable in all patients. Moreover, CRB1-09, CRB1-12, and CRB1-13 performed the BCVA test using eccentric vision. The few obtained values showed no correlation with disease duration or age ($r = -0.25$, $P = 0.6$; data not shown). Visual field was measurable in only three patients. The thresholds for blue light showed a strong correlation with disease duration ($r = 0.87$), whereas the thresholds for red light showed a weaker correlation ($r = 0.65$; Fig. 1A). Both thresholds rose during the disease progression. The correlation was weaker if the FST values were correlated with age instead of disease duration ($r = 0.77$ for blue light, $r = 0.57$ for red light, data not shown).

For the blue–red difference in the FST threshold, there was a clear increase with disease duration with a correlation of $r = 0.8$ (Fig. 1B), whereas only patients in the late stages beyond 30 years of disease duration approached the blue–red difference of zero indicating a pure cone-based vision. The blue–red differences correlated less strongly with age ($r = 0.71$, data not shown).

The MRAs as well as the PIPRs for red and blue light were averaged over both eyes for each patient. The MRA showed a small reduction with the disease duration in either color with a low correlation ($r = -0.55$ for blue, $r = -0.3$ for red); however, this correlation did not reach statistical significance (Fig. 2). The correlation did not change relevantly if MRAs were correlated with age instead of disease duration ($r = -0.6$ for blue, $r = -0.22$ for red; data not here).

The difference in the PIPR between blue and red stimulation showed no correlation either with disease duration or age ($r = -0.05$ for disease duration [Fig. 3] and $r = -0.2$ for age [data not shown]).

Comparison of the Pupil Response Results between Patients With Biallelic *CRB1* Variants and Healthy Eyes

Average pupil response curves differed from the age-matched norm values for blue and red stimuli (Fig. 4). The maximal relative constriction amplitudes were reduced for red and blue light.

MRAs were significantly smaller in the *CRB1* cohort than in the normal age-matched population ($P < 0.001$, Fig. 5).

The difference PIPR blue – PIPR red as a parameter of the inner retinal function was significantly increased for the *CRB1* patient group compared to that in age-matched healthy controls ($P = 0.003$, Fig. 6).

Genetic Findings

All patients in our cohort carried biallelic putative pathogenic variants in the *CRB1* gene. The genotypes are listed in Table 1, and the pathogenicity predictions for the missense variants are shown in Table 2. Segregation analysis was not possible in patient CRB1-02. Therefore biallelism could not be formally proven in this case. We considered all variants in Table 2 to be pathogenic, except for the p.S638S variant. This variant was seen in the compound

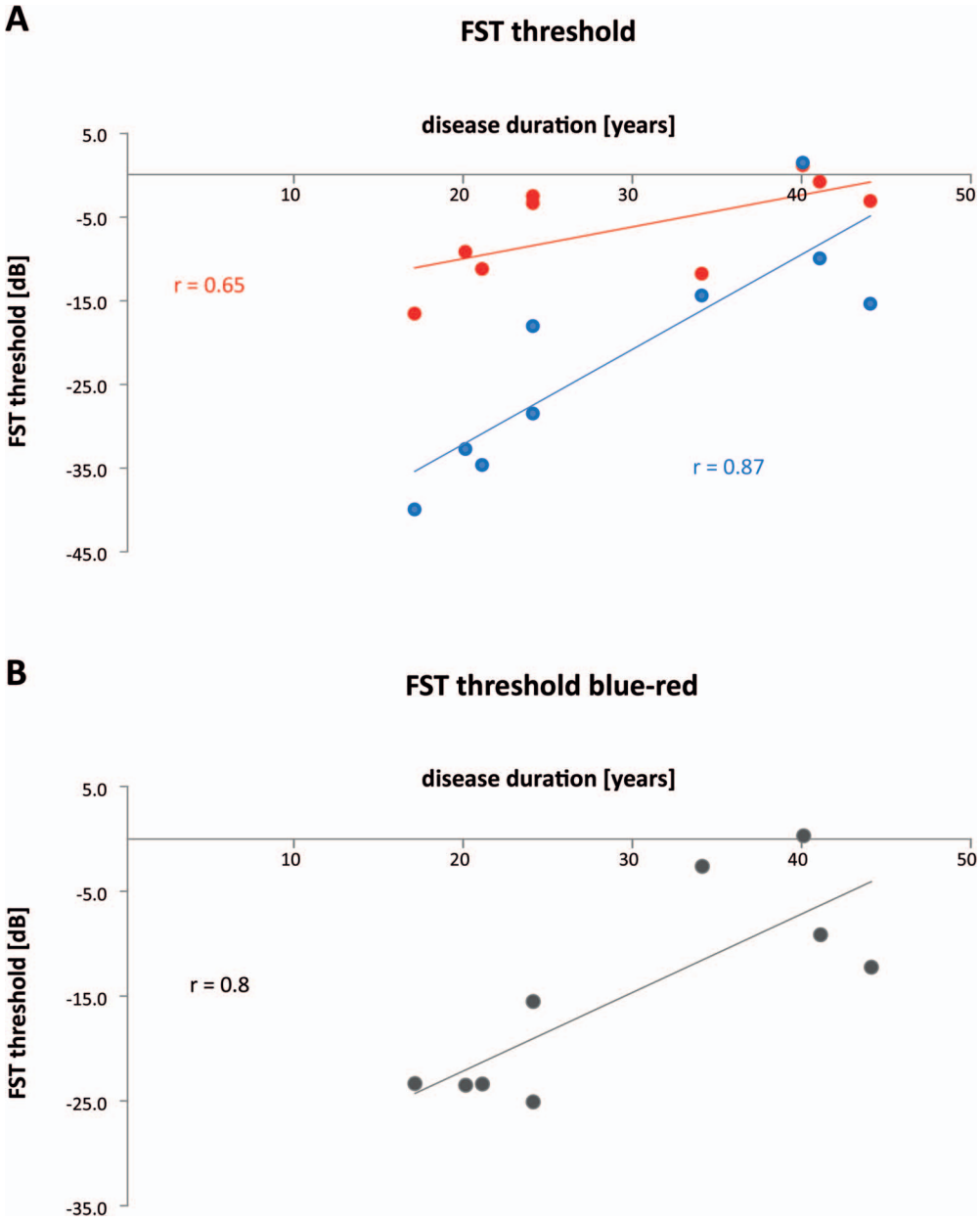

Figure 1. Correlation of the FST thresholds with the individual disease duration. (A) Correlation of the FST threshold values in dB on the *y*-axis (as defined from the baseline of 0 dB = 0.01 cd/m^2) with disease duration in years on the *x*-axis. Values for the FST test with blue and red light are shown in the corresponding colors. (B) Correlation of the FST blue–red threshold difference in dB averaged from both eyes per subject with disease duration in years.

heterozygous state with a 1-bp deletion in patient CRB1-05. In silico analysis of the p.S638S variant using two splice site prediction algorithms embedded in the Human Splicing Finder version 3.1[27] revealed no significant difference between mutant and reference sequence. However, since the variant is not listed in the Genome Aggregation Database (gnomAD) Version r2.0.2,[28] it seems to be extremely rare, if not private, and might execute a splicing defect that could not be predicted by the algorithms we used. Because the counter allele in patient CRB1-05 is a true loss–of-function allele, the contribution of a hypomorphic allele would be sufficient to explain the phenotype.

Discussion

RP caused by autosomal recessive *CRB1* mutations typically is an early-onset disease with its first

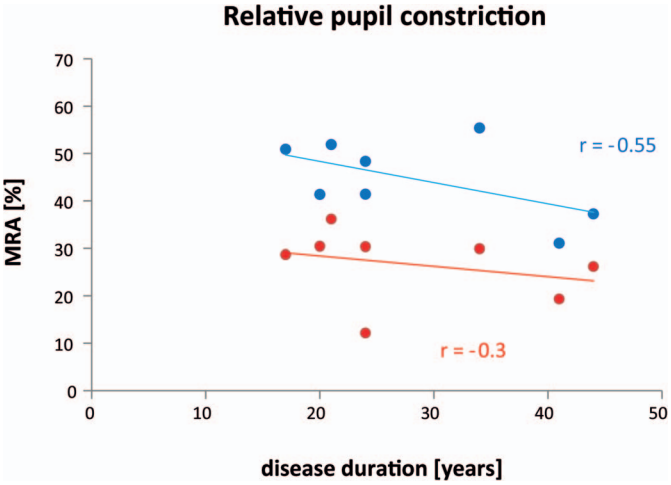

Figure 2. Correlation of the MRA (%; *y*-axis) with disease duration (years; *x*-axis). Values for the tests with blue and red light are shown in the corresponding colors.

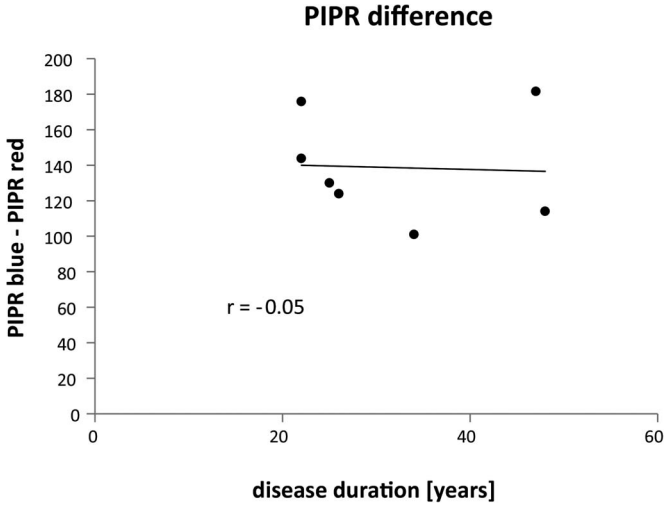

Figure 3. Correlation of the PIPR difference (blue–red) with disease duration.

manifestation before school age. As usual with EORDs, progress often is more rapid than in most retinal degeneration cases with later onset; thus, classical clinical follow-up functional diagnostics, such as perimetry or electroretinography, are no more reliably measurable in young adult years.[1,9,10]

In this study, we included only patients with early-onset RP due to biallelic *CRB1* mutations into the analysis. Other phenotypes, such as cone or cone-rod degenerations with early macular edema,[13,14] or macular degeneration due to *CRB1* mutations,[3] were not part of this cohort because they present a different subtype of the *CRB1* phenotype.

In our cohort, the four patients with the shortest disease duration (17, 20, 21, and 34 years) had a measurable visual field, whereas the largest visual field area belonged to the one with the shortest disease duration of 17 years. Although these findings confirmed that perimetry is a valid clinical progression marker in RP, its clinical relevance disappears in the early adult age in the cohort with *CRB1* mutations due to the fast progression. Similarly, the few values of measurable visual acuity did not correlate strongly with disease duration, but this result might be due to underpowered data (only six patients); the remaining patients did not have a reliably measurable visual acuity.

In general, functional follow ups in the late stages of retinal degenerations are a challenge for functional diagnostics. Following outer retinal degeneration, functionality of the inner retina is not well accessible for functional tests. This becomes a challenge for novel therapies for inherited retinal degenerations.[29–32] We showed here that the responses to blue light measured by FST testing may be a valid marker for functionality decline and disease progression in patients with *CRB1* variants in stages up to more than 40 years of disease duration. In the oldest patient of 56 years, even this subjective dark-adapted blue light threshold by FST could no longer be measured due to extremely low retinal sensitivity: the patient could not see any light in the test setting. We showed that the subjective test of the dark-adapted threshold to blue light correlates better with the individual disease duration than with age, indicating that the slightly different onset of the symptoms might be more relevant for progression than the objective age. The difference in the blue and red thresholds is a parameter indicating whether rod-based, dark-adapted vision is available: a difference that is significantly different from zero is a sign of rod-based vision; differences below 5 dB prove a cone-driven function; if the difference is 20 dB or more, it is rod-driven.[19] In this cohort, rod-based vision was clearly available for the younger part of the cohort (with disease duration up to 24 years; these patients were younger than 27 years), patients a with disease duration of more than 30 years approached values around zero. This shows that some residual rod function is present in the retina in later stages of *CRB1*–associated RP even as late as 30 years after the first symptom onset. Moreover, these results showed that the FST measurement could provide measurable outcomes in patients with no remaining visual field.

An additional test that can provide measurable results in the late stages of RP is analyzing pupil responses to full-field stimulation with blue or red

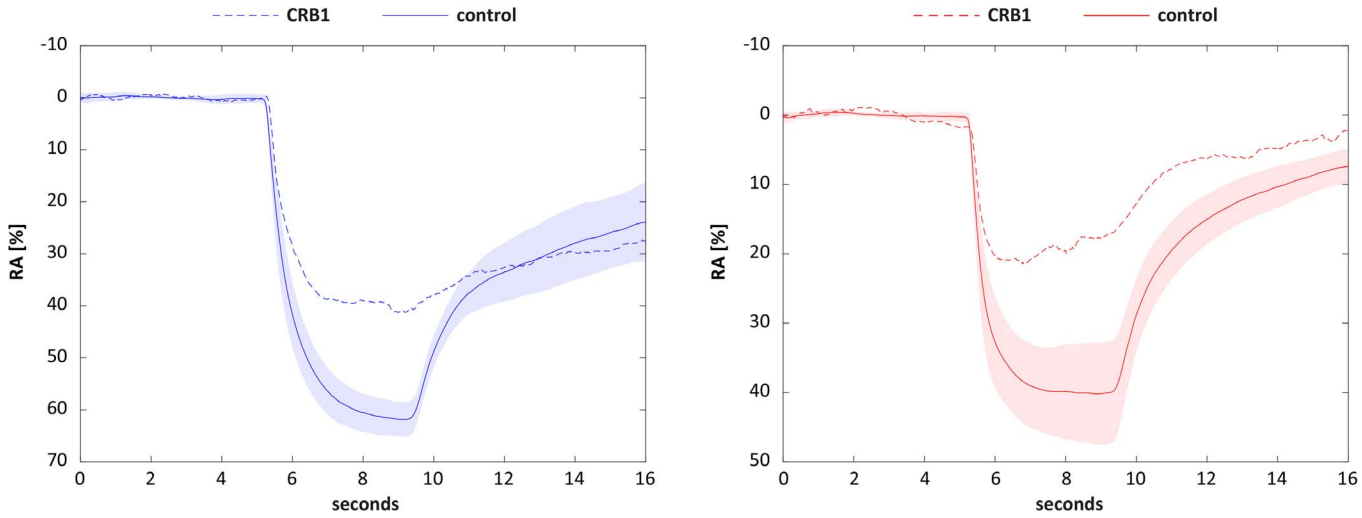

Figure 4. Averaged pupillary response curves for healthy eyes (*full line*) and *CRB1* patients (*dashed line*) for blue and red stimuli (stimulus duration 4 seconds from time point 5–9 seconds).

light.[20] These responses are objective, in contrast to FST responses, where the patient is asked to respond by the trigger button. The pupil responses provide some more insight into the progression of retinal degeneration. An important, although expected finding is the reduction of the MRA for red and blue full-field stimulation in patients with *CRB1* variants compared to age-matched normal eyes, a finding that is consistent with our previous examinations of RP patients independent of gene mutation[17] and the results from other groups.[33–35] This reduction of the pupil responses is a result of the degeneration of the photoreceptor layer, and possibly also the partial degeneration of ganglion cells. We could not observe the same strong correlation of the functional decline as in the FST subjective dark adaptation thresholds over the disease duration.

In general, the pupil response is a combination of multiple contributions from cones, rods and melanopsin-mediated direct activation of intrinsically photosensitive retinal ganglion cells (ipRGCs). Thus, even when most photoreceptors are degenerated, there is a residual pupil response driven by the ipRGC activity. Similar to a previously reported cohort of patients with LCA and EORD carrying *RPE65* variants,[35] the PIPR—a sign of ipRGCs activity—was larger in the *CRB1* than in the control

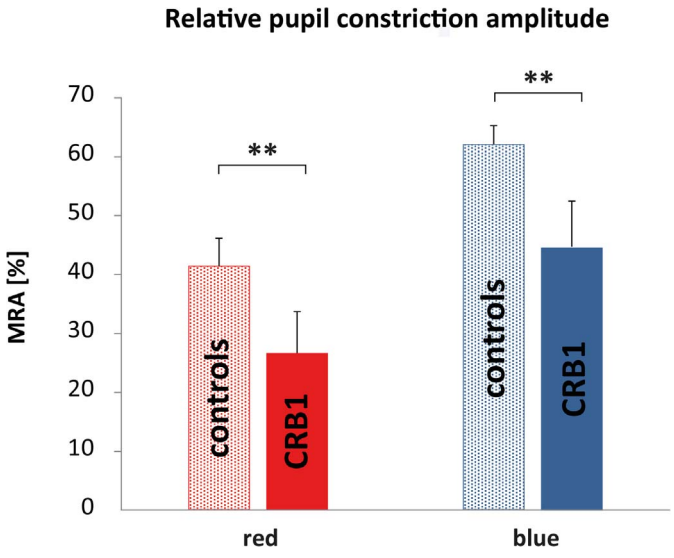

Figure 5. MRAs for healthy age-matched control eyes (*light colored bars* with standard deviations) and patients carrying *CRB1* mutations (*dark colored bars* with standard deviations) to red and blue full-field stimulation differ significantly ($P < 0.001$).

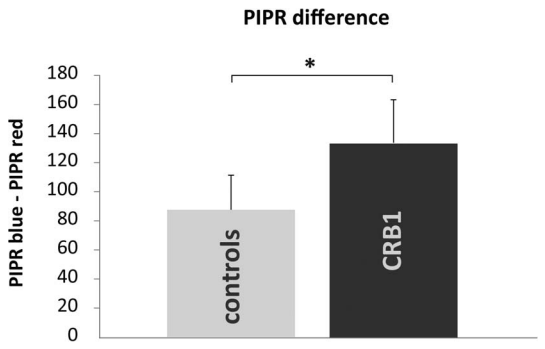

Figure 6. The difference in the PIPR between blue and red stimulation (blue–red) was significantly increased in the cohort with *CRB1* mutations (*black bar* with standard deviation) compared to that in the age-matched normal population (*gray bar* with standard deviation).

groups. This can be interpreted in several ways. First, the inner retinal function remains preserved (as far as ipRGC signaling is concerned). Secondly, the lack of inhibitory signals from blue cones may even increase this parameter. This was already speculated in previous publications.[17,20] Additionally, this lack of inhibitory signal could explain the observed difference between the baseline pupil size between controls and *CRB1* patients. Thus, because several factors exist with possibly opposite effects on the amplitude of pupil responses, it is not surprising that we could not find a linear correlation between the disease duration and MRA.

We observed no change in of the PIPR difference (blue–red) over the disease duration. We speculated that the function of inner retina, despite some morphologic changes, is preserved during disease progression. This information is critically important to implement new emerging therapeutic approaches. In patients with *CRB1* mutations, in particular, the inner retina is thickened compared to the healthy retina.[8] It has been proposed that this thickening may reflect a functionality loss, because the thickened inner retina resembles an immature tissue. However, a good retinal function in the early years of most patients as well as our PIPR results indicated that this may not necessarily be true for the remaining inner retina even after progressed outer retinal degeneration. The OCT imaging showed *CRB1*-associated thickening of the retina in all patients, as reported in the literature.

Interestingly, the maximal relative pupil constriction amplitude to cone-favoring stimuli (red stimuli) showed no dependence on the disease duration. However, we found a clear difference between the groups carrying *CRB1* variants and healthy controls in this value; namely, a reduction of the pupil responses in the patient cohort. This indicated that this change already has been present in the early phase of the disease and remained relatively stable. We could speculate that the pathologic morphogenesis and maturation of the retina in the *CRB1* phenotype[1,8] leads to an early functional problem of the cones that does not deteriorate rapidly over the life decades. However, because our population included patients with >10 years disease duration, this assumption is only speculative. Additionally, the cross-sectional nature of this study presents a limiting factor in predicting the functional progression in early-onset RP caused by biallelic *CRB1* mutations.

An interesting finding in this cohort is the strong correlation of the visual acuity with the red FST thresholds. This correlation must be considered cautiously, because the very low values of the BCVA are not reliably measurable and were gained via different test methods: Snellen acuity or BRVT or via logMAR estimation based on previous publications.[26]

Two of our patients with an EORD due to the *CRB1* genotype were excluded from the analysis due to glaucoma. Scant literature supports a glaucoma association with the *CRB1* gene. Henderson et al.[36] described that two of 41 patients with a *CRB1* retinal dystrophy had seclusio pupillae and secondary glaucoma due to peripheral retinal telangiectasia. Our patient CRB1-06 suffered angle-closure glaucoma in both eyes at the age of 56 years due to cataract. Patient CRB1-14 had also angle-closure glaucoma on both eyes at the age of 40 years. This patient also presented with corneal opacities and suspected keratoconus. Because glaucoma can change retinal function, we excluded these patients from analysis because we had insufficient evidence to state that glaucoma would be a feature strongly associated with the *CRB1* phenotype.

Conclusions

Full-field stimulus threshold with blue light as well as the blue–red difference of the thresholds have the potential to be a valid clinical progression marker in early-onset RP caused by biallelic *CRB1* mutations even in late stages with no detectable visual field. The pupil responses to full-field chromatic stimuli show significant differences to those in a normal population; the remaining responses, although reduced, indicated a partially preserved inner retinal function, despite severe photoreceptor dysfunction. Confirmation of these results and conclusions is necessary through longitudinal studies.

Acknowledgments

Supported by the Egon Schumacher-Stiftung, Germany and the Center for Personalized Medicine, Medical Faculty, University of Tübingen; the Curing Retinal Blindness Foundation and the Candle in the Dark–Child Vision Research Fund, managed by the King Baudouin Foundation (FPMC and MIK); the Algemene Nederlandse Vereniging ter Voorkoming van Blindheid and Landelijke Stichting voor Blinden en Slechtzienden that contributed through UitZicht 2014-13, together with the Rotterdamse Stichting Blindenbelangen, Stichting Blindenhulp and the

Stichting tot Verbetering van het Lot der Blinden (FPMC).

Disclosure: **K.T. Stingl**, None; **L. Kuehlewein**, None; **N. Weisschuh**, None; **S. Biskup**, None; **F.P.M. Cremers**, None; **M.I. Khan**, None; **C. Kelbsch**, None; **T. Peters**, None; **M. Ueffing**, None; **B. Wilhelm**, None; **E. Zrenner**, None; **K. Stingl**, None

References

1. Bujakowska K, Audo I, Mohand-Saïd S, et al. CRB1 mutations in inherited retinal dystrophies. *Hum Mutat*. 2012;33:306–315.
2. den Hollander AI, Audo I, Mohand-Saïd S, et al. Mutations in a human homologue of Drosophila crumbs cause retinitis pigmentosa (RP12). *Nat Genet*. 1999;23:217–221.
3. Khan KN, Robson A, Mahroo OAR, et al. A clinical and molecular characterisation of CRB1-associated maculopathy. *Eur J Hum Genet*. 2018; 26:687–694.
4. Tepass U, Theres C, Knust E. crumbs encodes an EGF-like protein expressed on apical membranes of Drosophila epithelial cells and required for organization of epithelia. *Cell*. 1990;61:787–799.
5. Pellissier LP, Lundvig DM, Tanimoto N, et al. CRB2 acts as a modifying factor of CRB1-related retinal dystrophies in mice. *Hum Mol Genet*. 2014;23:3759–3771.
6. Pellissier LP, Alves CH, Quinn PM, et al. Targeted ablation of CRB1 and CRB2 in retinal progenitor cells mimics Leber congenital amaurosis. *PLoS Genet*. 2014;9:e100397.
7. Mehalow AK, Kameya S, Smith RS, et al. CRB1 is essential for external limiting membrane integrity and photoreceptor morphogenesis in the mammalian retina. *Hum Mol Genet*. 2003; 12:2179–2189.
8. Jacobson SG, Cideciyan AV, Aleman TS, et al. Crumbs homolog 1 (CRB1) mutations result in a thick human retina with abnormal lamination. *Hum Mol Genet*. 2003;12:1073–1078.
9. Mathijssen IB, Florijn RJ, van den Born LI, et al. Long-term follow-up of patients with retinitis pigmentosa type 12 caused by CRB1 mutations: a severe phenotype with considerable interindividual variability. *Retina* 2017;37:161–172.
10. Papadopoulou Laiou C, Preising MN, Bolz HJ, Lorenz B. [Genotype-phenotype correlations in patients with CRB1 mutations]. *Klin Monatsbl Augenheilkd*. 2017;234:289–302.
11. McKay GJ, Clarke S, Davis JA, Simpson DAC, Silvestri G. Pigmented paravenous chorioretinal atrophy is associated with a mutation within the crumbs homolog 1 (CRB1) gene. *Invest Ophthalmol Vis Sci*. 2005;46:322–328.
12. Talib M, van Schooneveld MJ, van Sexen MM, et al. Genotypic and phenotypic characteristics of CRB1-associated retinal dystrophies: a long-term follow-up study. *Ophthalmology*. 2017;124:884–895.
13. Morarji J, Lenassi E, Black GCM, Ashworth JL. Atypical presentation of CRB1 retinopathy. *Acta Ophthalmol (Copenh)*. 2016;94:e513–514.
14. Khan AO, Aldahmesh MA, Abu-Safieh L, Alkuraya FS. Childhood cone-rod dystrophy with macular cystic degeneration from recessive CRB1 mutation. *Ophthalmic Genet*. 2014;35:130–137.
15. Hettinga YM, van Sexen MM, Wieringa W, Ossewaarde-van Norel J, de Boer JH. Retinal dystrophy in 6 young patients who presented with intermediate uveitis. *Ophthalmology*. 2016;123: 2043–2046.
16. Weisschuh N, Mayer AK, Strom TM, et al. Mutation detection in patients with retinal dystrophies using targeted next generation sequencing. *PLoS One*. 2016;11:e0145951.
17. Kelbsch C, Maeda F, Lisowska J, et al. Analysis of retinal function using chromatic pupillography in retinitis pigmentosa and the relationship to electrically evoked phosphene thresholds. *Acta Ophthalmol. (Copenh)*. 2017;95:e261–e269.
18. Bailey IL, Jackson AJ, Minto H, Greer RB, Chu, MA. The Berkeley rudimentary vision test. *Optom Vis Sci Off Publ Am Acad Optom*. 2012; 89:1257–1264.
19. Roman AJ, Cideciyan AV, Aleman TS, Jacobson, SG. Full-field stimulus testing (FST) to quantify visual perception in severely blind candidates for treatment trials. *Physiol Meas*. 2007;28:N51–N56.
20. Kelbsch C, Maeda F, Strasser T, et al. Pupillary responses driven by ipRGCs and classical photoreceptors are impaired in glaucoma. *Graefes Arch Clin Exp Ophthalmol*. 2016;254:1361–1370.
21. Weisschuh N, Feldhaus B, Khan MI, et al. Molecular and clinical analysis of 27 German patients with Leber congenital amaurosis. *PLoS One*. 2018;13:e0205380.
22. Kumar P, Henikoff Is, Ng PC. Predicting the effects of coding non-synonymous variants on protein function using the SIFT algorithm. *Nat Protoc*. 2009;4:1073–1081.

23. Adzhubei IA, Schmidt S, Peshkin L, et al. A method and server for predicting damaging missense mutations. *Nat Methods*. 2010;7:248–249.
24. Schwarz JM, Cooper DN, Schuelke M, Seelow, D. MutationTaster2: mutation prediction for the deep-sequencing age. *Nat Methods*. 2014;11:361–362.
25. Choi Y, Chan AP. PROVEAN web server: a tool to predict the functional effect of amino acid substitutions and indels. *Bioinforma*. 2015;31:2745–2747.
26. Lange C, Feltgen N, Junker B, Schulze-Bonsel K, Bach M. Resolving the clinical acuity categories "hand motion" and "counting fingers" using the Freiburg Visual Acuity Test (FrACT). *Graefes Arch Clin Exp Ophthalmol*. 2009;247:137–142.
27. Desmet F-O, Hamroun D, Lalande M, Collod-Béroud G, Claustres M, Béroud C. Human Splicing Finder: an online bioinformatics tool to predict splicing signals. *Nucleic Acids Res*. 2009;37:e67.
28. Lek M, Karczewski KJ, Minikel EV, et al. Analysis of protein-coding genetic variation in 60,706 humans. *Nature*. 2016;536:285–291.
29. Stingl K, Zrenner E. Electronic approaches to restitute vision in patients with neurodegenerative diseases of the retina. *Ophthalmic Res*. 2013;50:215–220.
30. Stingl K, Schippert R, Bartz-Schmidt KU, et al. Interim results of a multicenter trial with the new electronic subretinal implant alpha AMS in 15 patients blind from inherited retinal degenerations. *Front Neurosci*. 2017;11:445.
31. Hardcastle AJ, Sieving PA, Sahel JA, et al. Translational retinal research and therapies. *Transl Vis Sci Technol*. 2018;7:8.
32. Simunovic MP, Shen W, Lin JY, Protti DA, Lisowski L, Gillies MC. Optogenetic approaches to vision restoration. *Exp Eye Res*. 2018;178:15–26.
33. Kardon R, Anderson SC, Damarjian TG, Grace EM, Stone E, Kawasaki A. *Ophthalmology*. 2011;118:376–381.
34. Kawasaki A, Crippa SV, Kardon R, Leon L, Hamel C. Characterization of pupil responses to blue and red light stimuli in autosomal dominant retinitis pigmentosa due to NR2E3 mutation. *Invest Ophthalmol Vis Sci*. 2012;53:5562–5569.
35. Lorenz B, Strohmayr E, Zahn S, et al. Chromatic pupillometry dissects function of the three different light-sensitive retinal cell populations in RPE65 deficiency. *Invest Ophthalmol Vis Sci*. 2012;53:5641–5652.
36. Henderson RH, Mackay DS, Li Z, et al. Phenotypic variability in patients with retinal dystrophies due to mutations in CRB1. *Brit J Ophthalmol*. 2011;95:811–817.